https://doi.org/10.5194/bg-2021-234
Preprint. Discussion started: 29 September 2021

Biogeosciences Discussions
Open Access
EGU

Methane accumulation affected by particulate organic carbon in upper Yangtze deep valley dammed cascade reservoirs, China

Yuanyuan Zhang [1, 2], Youheng Su [2, 3], Zhe Li [1, 2*], Shuhui Guo[4], Lunhui Lu [1, 2], Bin Zhang [2], Yu Qin [3]

[1] College of Resources and Environment, Chongqing School, University of Chinese Academy of Sciences, 400714, Chongqing, China

[2] CAS Key Lab of Reservoir Environment, Chongqing Institute of Green and Intelligent Technology, Chinese Academy of Sciences, 400714, Chongqing, China

[3] College of River and Ocean Engineering, Chongqing Jiaotong University, 400074, Chongqing, China

[4] Foreign Environmental Cooperation Center, Ministry of Ecology and Environment of the People's Republic of China, 100035, Beijing, China

Corresponding author:
Email: lizhe@cigit.ac.cn

https://doi.org/10.5194/bg-2021-234
Preprint. Discussion started: 29 September 2021


Biogeosciences Discussions

Abstract

Methane (CH_4) emissions from freshwaters to the atmosphere have a profound impact on global atmospheric greenhouse gas (GHG) concentrations. Anthropogenic footprints such as dam construction and reservoir operation significantly changed the fate and transport of CH_4 in freshwaters. The type of particulate organic carbon (POC) in reservoirs is a critical factor controlling CH_4 production and emissions. However, little is known of how reservoir operation mediates the distribution of POC and regulates CH_4 accumulation in cascade hydroelectric reservoirs. Here, spatial and temporal variations in POC and CH_4 were explored in the Xiluodu (XLD) and Xiangjiaba (XJB) reservoirs which are deep valley dammed cascade reservoirs located in the main channel of the upper Yangtze River. Based on the δ^{13}C-POC and N/C mole ratios of particulate organic matter, the results of multi-endmember stable isotope mixing models by a Bayesian model show that terrestrial POC and autochthonous POC accounted for approximately 56 ± 19% and 42 ± 19% (SD, n=181) of POC, respectively. CH_4 concentrations and δ^{13}C-CH_4 in the cascade reservoirs were potentially influenced by CH_4 oxidation. Together with other physicochemical parameters and structural equation model, these results suggested that the input of terrestrial POC was dominantly influenced by water level variations and flow regulation due to reservoir operation. The cumulative effect of POC caused by cascade reservoirs was not apparent at a bimonthly scale. Terrestrial POC was more likely to dominate CH_4 accumulation in cascade reservoirs under reservoir operation.

https://doi.org/10.5194/bg-2021-234
Preprint. Discussion started: 29 September 2021


Biogeosciences Discussions Open Access EGU

1 Introduction

Methane (CH_4) is widely recognized as the second most important greenhouse gas after carbon dioxide (CO_2) (Saunois et al., 2020). The latest data shows that global atmospheric CH_4 was 1888.5 ppb in July 2021 (Dlugokencky, 2021). The annual increase in global atmospheric CH_4 between 2007 and 2020 fell within the range of 7.99 ppb·yr^{-1} to 14.81 ppb·yr^{-1} (Dlugokencky, 2021). Global CH_4 emissions were estimated to be up to 579 Tg. yr^{-1} from 2008 to 2017 (Saunois et al., 2020). There is a very high level of confidence that the atmospheric CH_4 increase during the Industrial Era was caused by anthropogenic activities, which caused approximately 60% CH_4 emissions (Ciais et al., 2014; Saunois et al., 2016; Saunois et al., 2020). However, not all the sources of global CH_4 emissions are explicitly and well explained. Although half of the global methane emissions come from the aquatic ecosystems (Rosentreter et al., 2021), a large proportion of the uncertainties in the global CH_4 budget arise from freshwater systems. The production of CH_4 in lakes and reservoirs is an important process in the global methane cycle. This is partly because freshwater systems are closely linked to and manipulated by anthropogenic activities, e.g., hydrological process regulation, geomorphological alternation, large inputs of organic carbon, and nutrients from surrounding communities. Anthropogenic footprints significantly change the fate and transport of CH_4 in freshwaters.

Dam construction and reservoir impoundments are widely accepted as important anthropogenic activities that significantly change the sink and sources of CH_4 in the freshwater systems. In general, the net change in CH_4 emissions in reservoirs is primarily contributed by the decomposition of organic matter (OM), e.g., soil organic carbon and vegetation cover, due to flooding. Reservoir CH_4 emissions may reach the highest levels immediately after impoundment and exponentially decline with aging (Abril et al., 2005). Second, the reduced flow velocity and increased hydraulic retention time (HRT) in the reservoir accumulates terrestrial OM from the upstream watershed to the reservoir bottom, supporting the development of anoxic habitats at the reservoir

https://doi.org/10.5194/bg-2021-234
Preprint. Discussion started: 29 September 2021

bottom for intensive methanogenesis. Site-specific hydro-morphological characteristics, reservoir thermal regimes, and external OM loads from the upstream watershed supported consistent reservoir CH_4 emissions. This evidence supported a wide acceptance that reservoirs consistently emit CH_4 that exceeds those of upstream reaches of the same river and, on average, from natural lakes (Stanley et al., 2016).

However, the role of dams and reservoirs in the global CH_4 budget has been received challenges in recent years. Previous studies reported that global reservoirs were either CH_4 neutral or CH_4 sources and that reservoir productivity and temperature are better predictors than reservoir age (Deemer et al., 2016). Reservoirs may reduce CH_4 and CO_2 emissions in downstream floodplain wetlands caused by upstream organic carbon (OC) transport and sedimentation (Muller, 2019). Sediment loads and nutrient enrichments were the primary and secondary driving factors that regulate CH_4 formation in navigable river impoundments (Wilkinson et al., 2019). While river impoundments did not account for all hotspots of CH_4 formation in their study, they implied that sediment management would offset CH_4 emissions from damming rivers (Wilkinson et al., 2019). The largest share of CH_4 emissions may be due to OC retention and mineralization in the reservoir (Shi et al., 2017). Recent research showed that imbalanced stoichiometric sedimentation mediated CH_4 accumulation in the mid-part of China's Three Gorges Reservoir (Li et al., 2020a). However, the findings supported that reservoir operation strategy significantly impacts the patterns of CH_4 accumulation. Growing research has highlighted the importance of reservoir hydrology and sediment (or OC) dynamics contributing to CH_4 accumulation and emissions. If reservoir operation could be proven to have an evident link with CH_4 dynamics and emissions, there would be best practices for the hydropower industry to reduce excessive CH_4 emissions, which is meaningful for mitigating the global warming potential of hydropower. However, the question of how reservoir operation mediates particulate organic carbon (POC) transport and finally impacts CH_4 dynamics and emissions from reservoir appears to be sophisticated and site-specific and has not been well addressed.

The study was extended from a single reservoir to a cascade system in the upper

https://doi.org/10.5194/bg-2021-234
Preprint. Discussion started: 29 September 2021

Yangtze River to explore dissolved CH_4 accumulation under reservoir operation. The research objectives are (1) to determine the input and accumulation of POC that influence dissolved CH_4 accumulation under the physiochemical parameters caused by cascade reservoir operation and (2) to explain how the different sources of POC regulate the dissolved CH_4 accumulation in deep river-valley dammed reservoirs.

2 Methods

2.1 Site description and sampling campaign

The Xiluodu (XLD) reservoir and Xiangjiaba (XJB) reservoir are two deep river-valley dammed cascade reservoirs located along the main channel of the upper Yangtze River, which is frequently referred to as the "Jinsha River" (Figure 1). Both the XLD and XJB hydro-projects serve as hydroelectricity production facilities. They also perform significant seasonal water level adjustments for flood control as their partial services (Figure 2). The initial impoundment of both reservoirs started in July 2013. XJB finished its impoundment in September 2013, while XLD finished its full impoundment one year later. The parameters of the XLD and XJB reservoirs are shown in Table S1 (Li et al., 2017b).

The sampling campaign was conducted every other month between January 2018 and January 2019. Fifteen sampling sites were located along the main channel of both reservoirs, L3 to L1 in the XLD reservoir, B10 to B1 in the XJB reservoir and X2 to X1 downstream of the XJB reservoir (Figure 1). Because it was not possible to cover all the sampling sites and finish sampling work in one day, each sampling event was limited between the dates of the 10th and 15th of that month. The sampling time of a day was controlled between 8:00 AM and 6:00 PM. In particular, the inconvenience of local transportation in such deep valley areas along the XLD reservoir limited sampling to 40 km upstream of the XLD dam, encompassing sampling sites L3 to L1. Downstream of the XJB, to avoid tributary disturbance to collected samples, the sampling work was limited within 10 km downstream of the XJB dam, encompassing sampling sites X2 and X1.

10 L water samples were collected at 0.5 m below the water surface and

https://doi.org/10.5194/bg-2021-234
Preprint. Discussion started: 29 September 2021

146 approximately 2 m above the sediment layer at each sampling site. However, in the river
147 reach right below both dams, where sites B10 to B8 and X2 to X1 were located, the
148 water column was well mixed and only surface water samples were collected. These
149 samples were then treated as representative of both surface and bottom samples in such
150 a fully mixed water column. The water temperature, dissolved oxygen (DO) and pH
151 were measured *in situ* by a calibrated YSI® Pro 2030 probe (YSI Inc., Ohio, USA).

152 Due to the different operation schemes of each reservoir, HRT was the
153 fundamental key variable structuring the aquatic ecosystem of both reservoirs and was
154 distinctive between the XLD and XJB reservoirs. A detailed calculation of HRT is
155 provided in the Supporting Information (Section S1.1). Considering 2018 as an example
156 (Figure S1), the annual average cumulative HRT in the XLD reservoir was 32.9 ± 20.6
157 days (mean ± SD), with the 1st and 3rd quartiles between 14.7 days and 46.4 days. In
158 the XJB reservoir, the corresponding data collected in 2018 was 15.8 ± 8.6 days, with
159 1st and 3rd quartiles between 6.9 days and 23.4 days. The spatial and temporal
160 variations in the cumulative HRT in the XLD and XJB reservoirs also showed that the
161 cumulative HRT was positively correlated with the water level and negatively
162 correlated with the flow and shortest in the flood season (Figure S2).

https://doi.org/10.5194/bg-2021-234
Preprint. Discussion started: 29 September 2021

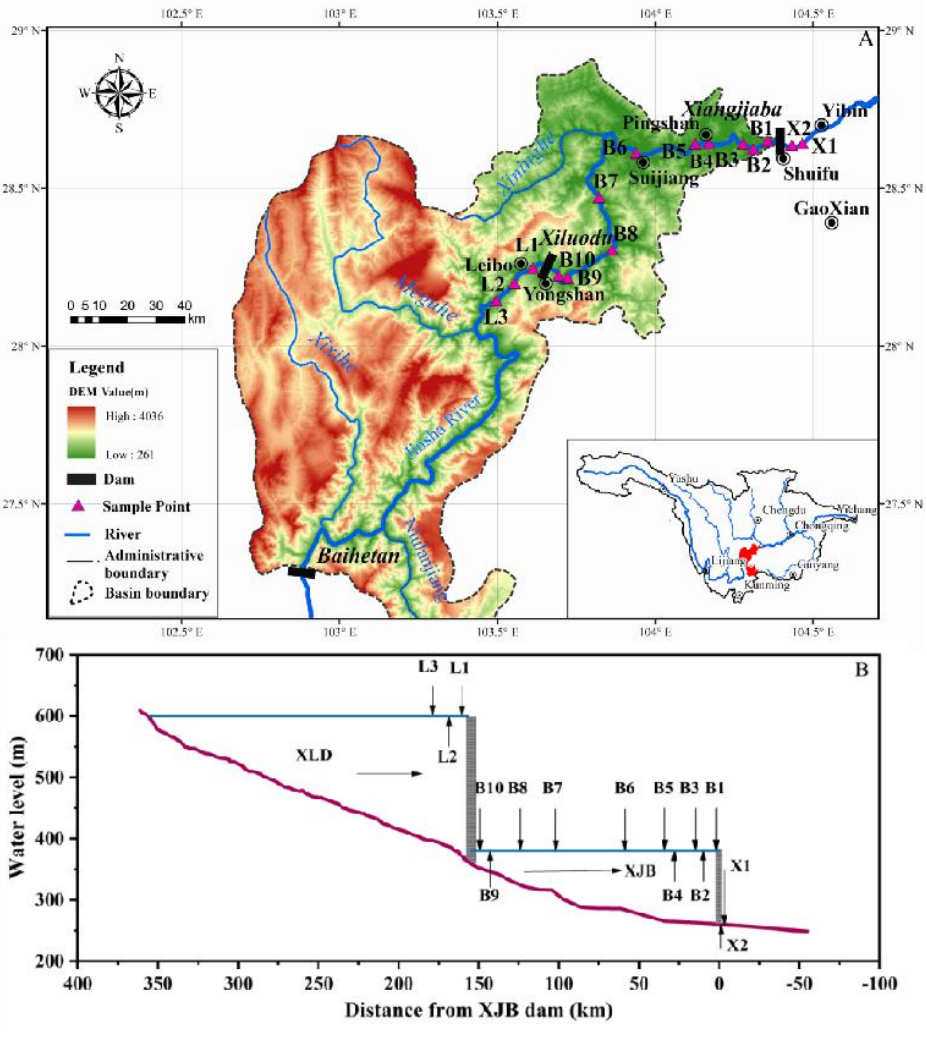

Figure 1. The Xiluodu (XLD) and Xiangjiaba (XJB) cascade reservoirs. A) the map of the two reservoirs and sketch of sampling sites; B) vertical profiles of the cascade reservoirs and location of the sampling sites.

https://doi.org/10.5194/bg-2021-234
Preprint. Discussion started: 29 September 2021

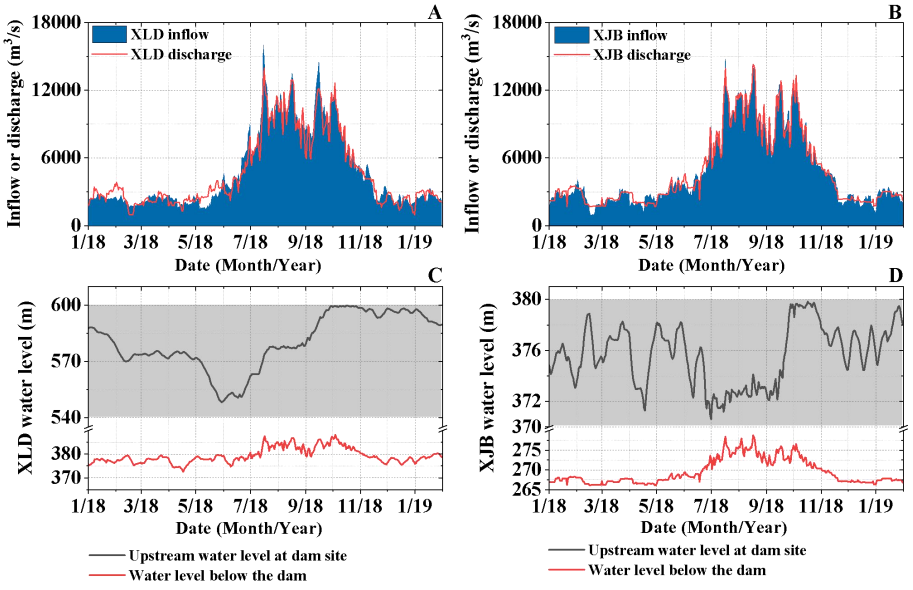

Figure 2. A) and B) daily reservoir inflow and discharge of the Xiluodu (XLD) and Xiangjiaba (XJB) reservoirs during the study; C) and D) daily water level variations at the upstream and downstream of the two dams. Daily reservoir inflow/discharge and water level variations of each reservoir were provided by the China Three Gorges Corporation (www.ctg.com.cn).

2.2 Measurement of CH_4 and CO_2 concentrations and other environmental parameters

CH_4 and CO_2 concentrations in the water phase were analyzed by the headspace approach (Unesco/Iha, 2010). Equipped with a Picarro® G2201-*i* Isotopic Analyzer (California, USA), our standard operation procedure was upgraded to the CH_4 and CO_2 headspace approach in 2017. Water samples were carefully collected by a 300 mL polypropylene syringe barrel and sealed underwater by its matching piston. Then, surplus water and possible air were ejected out carefully until the water sampling was 200 mL in the syringe. Then, 100 mL of highly purified nitrogen was sucked into the syringe and shaken immediately on-site for 2 minutes for gas exchange. Then, 100 mL gas samples were injected into pre-purified air sampling bags (0.3 L, HEDE tech, Dalian, China) for further analysis by Picarro® G2201-*i* Isotopic Analyzer under HP mode. Triplicates were performed for quality control.

For dissolved nutrients, water samples were filtered through pretreated (combusted

https://doi.org/10.5194/bg-2021-234
Preprint. Discussion started: 29 September 2021

at 450 °C for 4 h in a muffle furnace and weighed after cooling) Whatman® GF/F glass fiber membranes (Whatman®, UK). Dissolved organic carbon (DOC) was then analyzed by a Shimadzu® TOC-V TOC analyzer (Shimadzu, Japan). Dissolved total nitrogen (DTN) and total phosphorus (DTP) were analyzed by the standard method (Wef and Apha, 2005).

For particulate matter, the chlorophyll a (Chl-a) concentration was measured spectrophotometrically after 90% cool acetone extraction. All residues on the GF/F glass fiber membranes were dried at 65 ℃ for 48 h and reweighed. The concentration of total particulate matter (TPM) in the water column was the quotient of the mass difference between the two weights and the volume of water samples used infiltration. The 65 °C dried fresh residues were also used for elemental composition analysis of C, and N. POC, particulate organic nitrogen (PON), δ^{13}C-POC and δ^{15}N-PON were measured by a Thermo Fisher ® Flash H T Elemental Analyzer for Isotope Ratio MS (Thermo Fisher Scientific, MA, USA). The standard reference materials were Vienna Pee Dee Belemnite for carbon and atmospheric N_2 for nitrogen. Triplicates were also performed for quality control.

2.3 Application of stable isotope mixing models

Fits Stable Isotope Mixing Models (SIMMs) were meant as a longer-term replacement to the previously widely used package SIAR (Stable Isotope Analysis in R) (Parnell et al., 2010). SIMMs were used to infer dietary proportions of organisms consuming various food sources from observations on the stable isotope values taken from the organisms' tissue samples. The proportional contribution of different sources of OM to a mixture was estimated by using stable isotope mixing models " SIMMs ", which are based on Bayesian methods (Parnell et al., 2010; Parnell et al., 2013).

The newest Simmr package of stable isotope mixing models was implemented in the R program (Version: 4.0.3) to estimate the contribution of different sources of POC. The contributions of different endmembers to POC were calculated by the δ^{13}C, δ^{15}N and N/C molar ratios of particulate organic matter (POM). To estimate the contribution

https://doi.org/10.5194/bg-2021-234
Preprint. Discussion started: 29 September 2021

of POC sources, the endmember values of C3 and C4 plants were set from references (Kendall et al., 2001; Wu et al., 2007; Jiang and Ji, 2013; Wang et al., 2014; Chen et al., 2018b; Deng et al., 2018; Xuan et al., 2019; Ru et al., 2020), and the endmember values of soil and plankton from the upper Yangtze River were sampled and analyzed in the field sampling campaign (Table 1). The 50% quantile values were the predicted values of the model. The contribution of terrestrial POC was obtained by C3 and C4 plants, coastal soil, and plankton as the contribution of autochthonous POC.

Table 1. $\delta^{13}C$, $\delta^{15}N$, N/C molar ratios of particulate organic matter (POM) from different endmembers

Endmember	$\delta^{13}C$-POM (‰)	$\delta^{15}N$-POM (‰)	N/C
C3 plant	-28.9 ± 1.6	1.8 ± 3.7	0.038 ± 0.019
C4 plant	-13.4 ± 1.0	2.4 ± 5.7	0.038 ± 0.019
Soil	-21.0 ± 2.0	4.6 ± 1.4	0.134 ± 0.022
Plankton	-26.8 ± 0.6	6.6 ± 1.8	0.184 ± 0.011

2.4 Data analysis

The structural equation model was performed using the Lavaan package in the R program to obtain the effects of different variables by verifying the theoretical model. Since the original data difficultly satisfied the normal distribution tested by Kolmogorov–Smirnov test, the maximum likelihood relaxation algorithm (MLR) was used as the estimator.

Data analyses and plotting (Kolmogorov–Smirnov test, linear regression, and one-way analysis of variance [ANOVA]) were performed using OriginPro® 2018 (OriginLab Corporation, MA, USA) and Statistical Product and Service Solutions (SPSS). In one-way ANOVA, differences between means and 50% quantile values were considered significant at $p < 0.05$. A detailed description of the mass balance approach of the POC and CH_4 in both reservoirs is provided in the Supporting Information (Section S1.1).

https://doi.org/10.5194/bg-2021-234
Preprint. Discussion started: 29 September 2021

3 Results

3.1 Physical limnology and major environmental parameters

The water temperature ranged from 12.45 °C to 25.9 °C and 13.6 °C to 26.3 °C in the XLD and XJB reservoirs, respectively. The thermal stratification patterns of both reservoirs are different (Figure S3A). Thermal stratification developed in the XLD reservoir in spring, e.g., March, and persisted throughout the whole summer. Metalimnion existed approximately 60 m below the water surface. With the increase in water level due to reservoir impoundment, together with the decrease in air temperature, thermal stratification gradually disappeared in November. In the XJB reservoir, weak thermal stratification was initiated in March, which supported its spring algal blooms (Figure S3C). However, because the upstream reservoir increased its discharge to prepare abundant reservoir capacity before the summer flood season, the XJB reservoir was fully mixed in May. Hypolimnion in the XJB reservoir was limited to approximately 150 m below the water surface in May and approached to 180 m below the water surface in July as the discharge of the XLD reservoir apparently increased. In September, the XJB reservoir was fully mixed.

The DO in all samples varied from 7.06 to 16.08 mg/L with a mean value of 9.23 ± 0.91 mg/L (SD, n=181). The DO of surface water was significantly higher than that of bottom water in the XJB reservoir due to algal blooms in March. Additionally, the DO of the XLD reservoir in the flood season was slightly lower than that in the dry season (Figure S3B). Although both reservoirs were impounded in less than a decade, the trophic status of both reservoirs is meso-oligotrophic. The chlorophyll a (Chl-a) concentrations varied widely, with values of 0.01–35.02 mg/m^3. The maximum Chl-a concentration in surface water during the study was found in the XJB reservoir. The diatom bloom initiated in late February and continued to April in the XJB reservoir. The Chl-a concentration in the XLD reservoir was below 15 mg/m^3 throughout the year (Figure S3C). The bloom-forming period of the XLD reservoir was approximately the same as that of the XJB reservoir.

https://doi.org/10.5194/bg-2021-234
Preprint. Discussion started: 29 September 2021

The DOC concentrations in all samples varied from 0.04 to 6.13 mg/L with an average value of 2.37 ± 1.24 mg/L (SD, n=175). The maximum DOC concentration was found between May and July, with a mean value of 3.94 ± 0.69 mg/L (SD, n=52), and the minimum average value was found in January (1.24 ± 0.75 mg/L, SD, n=45, Figure S3D). There was no obvious spatial difference in DOC concentrations between the two reservoirs, which indicates that the DOC concentrations may be significantly affected by the input of upstream. In all the sampling sites, the TN and TP in the water column were 146.78 ± 64.6 μM (SD, n=182) and 2.51 ± 1.12 μM (SD, n=156), respectively. The mole ratio of TN: TP, as an indicator of nutrient limitation, fell in a range between 42.93 (1st quartile) and 91.84 (3rd quartile), indicating heavily P limitation for primary producers in both reservoirs.

3.2 Particulate organic matter and stable isotopic signatures

The TPM concentrations in all sampling sites of both reservoirs varied from 1.10 to 38.80 mg/L with a mean of 5.74 ± 5.03 mg/L (SD, n=182), and the average maximum TPM concentration was found in July and September with a value of 10.78± 4.34 mg/L (SD, n=52). The POC concentrations in all water samples varied from 0.03 to 2.81 mg/L with a mean of 0.35 ± 0.39 mg/L (SD, n=182, Figure 3). The PON concentrations in all samples ranged from 0.01 to 0.21 mg/L, with a mean of 0.04 ± 0.03 mg/L, and the N/C mole ratios varied from 0.019 to 0.273, with an average value of 0.116 ± 0.032 (SD, n=182, Figure 3). The maximum POC and PON concentrations and minimum N/C mole ratios were found in March, with average values of 0.98 ± 0.64 mg/L, 0.07 ± 0.05 mg/L and 0.079 ± 0.052, respectively (SD, n=26, Figure 3). Meanwhile, the maximum POC and PON concentrations in the surface and bottom water were found before the XJB dam, and the N/C mole ratios from upstream were lower than those downstream during this period. In particular, the values in the surface water were different from those in the bottom water, which may be due to the lower flow and temperature stratification (Figure 3A, 3B).

https://doi.org/10.5194/bg-2021-234
Preprint. Discussion started: 29 September 2021

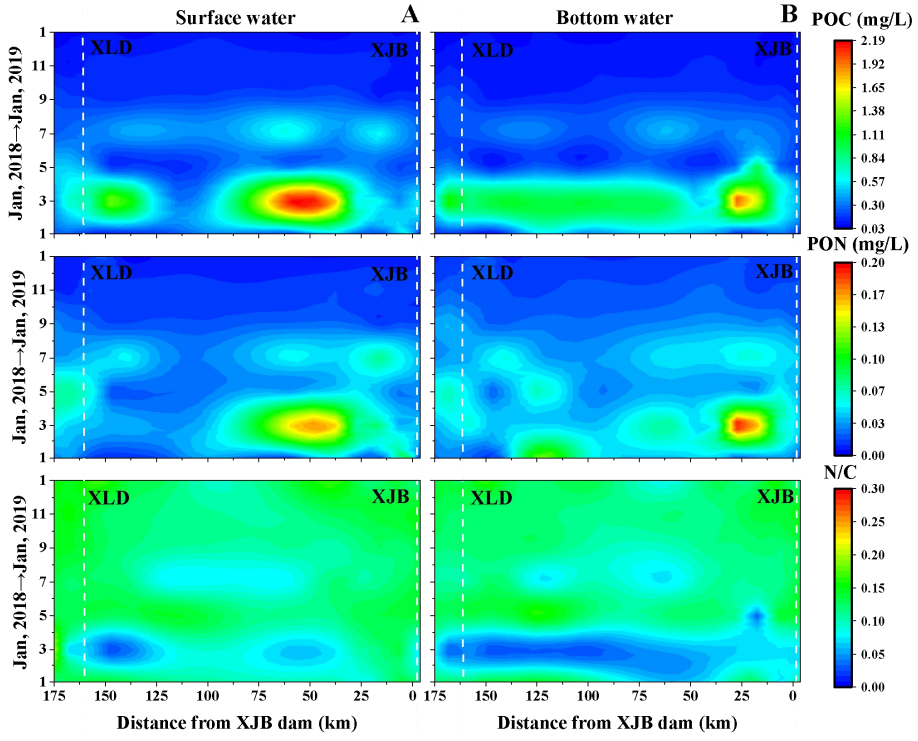

Figure 3. Wavelet figure showing the spatial and temporal distributions in particulate organic carbon (POC), particulate organic nitrogen (PON), and N/C mole ratios of particulate organic matter of the surface (A) and bottom (B) water from the XLD and XJB reservoirs.

The stable isotopic ratios and N/C mole ratios of POC and PON reveal that POM originated from different sources in the XLD and XJB reservoirs. Most δ^{13}C-POC values in all samples showed no significant differences during the year ranging between −13.0‰ and −35.3‰, with a mean of −26.1 ± 1.8‰ (SD, n=181). However, δ^{13}C-POC in March showed obvious differences that were higher than other values (−24.3 ± 3.3‰, SD, n=26). δ^{15}N-PON varied from −1.5‰ and 17.5‰ with a mean of 6.5 ± 2.7‰ (SD, n=182) which displayed irregularly high values in January 2018 (8.9 ± 4‰, SD, n=26). This may be influenced by the inputs of excrement or other anthropogenic activities during this period.

As shown in Figure 4A to Figure 4C, most POM in the XLD and XJB reservoirs may have been derived from plankton. However, the δ^{15}N-PON, which may be affected by trophic levels in the two reservoirs displayed large fluctuations (Chen et al., 2018a).

https://doi.org/10.5194/bg-2021-234
Preprint. Discussion started: 29 September 2021


Biogeosciences Discussions Open Access EGU

Thus, the N/C mole ratios of POM and δ^{13}C-POC can better constrain the contribution of different sources of POC in this study. As the average δ^{13}C-POC (−26.1‰) and N/C mole ratios of POM (0.116) were similar to those of plankton, with values of −26.8‰ and 0.184 respectively (Table 1), POC in the XLD and XJB reservoirs may have been primarily from plankton (42 ± 19%) and secondarily, from C3 plants (34 ± 16%) and less from soil (13 ± 11%) and C4 plants (8 ± 9%) (SD, n=181) (Figure 4D). Previous studies have reported that particulate matter derived from erosion of soil may have low OC adsorption due to the low clay content of surface soils in the Jinsha River Basin (Wu et al., 2020), which agrees with the results of this study. Conversely, the POC/Chl-a threshold ratio of 300 indicates the dominance of phytoplankton in the POC pool (Suzuki et al., 2014; Kang et al., 2019; De Castro Bueno et al., 2020), and more than half of the samples in the surface water were classified with the origin of phytoplankton dominance (Figure S4), which is similar to the results of stable isotope mixing models. POC can be divided into autochthonous and terrestrial POC. Autochthonous POC mostly originates from plankton, yet terrestrial POC derives from plants and soil in the catchment (Guillemette et al., 2013; Chen et al., 2018b; Tittel et al., 2019). The concentrations of autochthonous and terrestrial POC provided in the Supporting Information (Section S1.2, Figure S5) were estimated by the contributions of plankton, soil, C3 and C4 plants.

https://doi.org/10.5194/bg-2021-234
Preprint. Discussion started: 29 September 2021

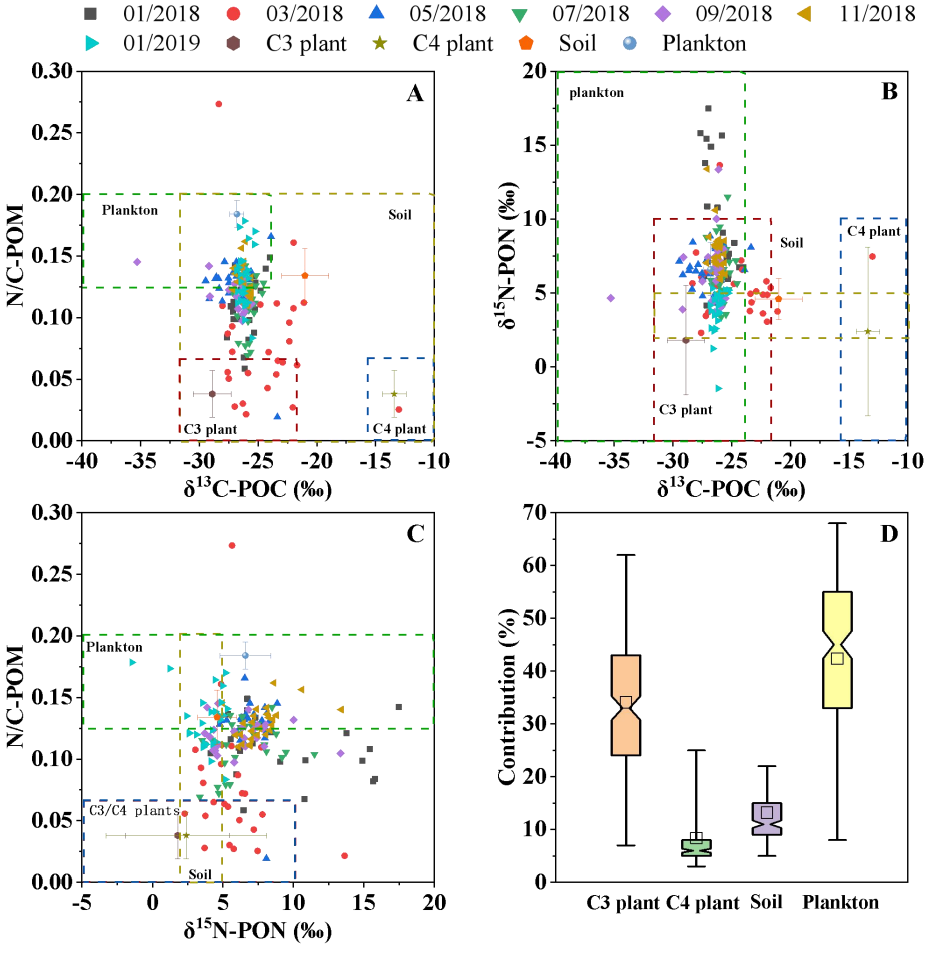

Figure 4. A) N/C mole ratios vs. δ^{13}C-POC, B) δ^{15}N-PON vs. δ^{13}C-POC, C) N/C mole ratios vs. δ^{15}N-PON in particulate organic matter (POM) and endmembers (C3 and C4 plants, soil, plankton) (the dotted area in A, B and C was from literature (Kendall et al., 2001)); D) the contribution of endmembers in the XLD and XJB reservoirs.

3.3 Spatial and temporal variations in CH_4 and CO_2 concentrations, δ^{13}C-CH_4

The annual CH_4 and CO_2 concentrations in all water samples from the two cascade reservoirs varied from 0.011 to 0.133 μmol/L and 0.016 to 0.257 mmol/L, with average values of 0.039 ± 0.024 μmol/L and 0.046 ± 0.025 μmol/L (SD, n=182), respectively. The annual average CH_4 concentration observed in the study was lower than those in global rivers and streams (1.45 ± 7.98 μmol/L, SD, n=1439) (Stanley et al., 2016). In XLD reservoir (L3–L1), annual CH_4 fell in a range between 0.014 μmol/L and

https://doi.org/10.5194/bg-2021-234
Preprint. Discussion started: 29 September 2021

0.052 μmol/L, with a mean of 0.026 ± 0.008 μmol/L during the study (SD, n=42) (Figure 5). Annual CO_2 in XLD reservoir fell in a range between 0.033 mmol/L and 0.092 mmol/L with a mean of 0.046 ± 0.017 mmol/L (SD, n=42) (Figure 5). In XJB reservoir (B10–B1), annual CH_4 fell in a range between 0.012 μmol/L and 0.133 μmol/L with a mean of 0.044 ± 0.026 μmol/L (SD, n=126). Correspondingly, annual CO_2 in the XJB reservoir fell in a range between 0.016 mmol/L and 0.257 mmol/L with a mean of 0.047 ± 0.028 mmol/L. Downstream of the XJB reservoir (X1–X2) had a range of CH_4 between 0.011 μmol/L and 0.064 μmol/L with a mean of 0.033 ± 0.016 μmol/L (SD, n=14). The water column CO_2 concentration downstream of the XJB reservoir was between 0.030 mmol/L and 0.077 mmol/L with a mean of 0.041 ± 0.013 mmol/L (SD, n=14). The longitudinal gradient of CH_4 concentration from upstream XLD reservoir to downstream XJB reservoir was evident, and the mid-part of the XJB reservoir (B6–B4) showed a relatively high level of CH_4 concentration among all samples. Comparatively, the longitudinal gradient of CO_2 concentration along the cascade reservoir was not apparent (Figure 5). The mole ratios between CH_4 and CO_2 (CH_4/CO_2) were among the highest in the middle of the XJB reservoir. For temporal variations, the highest CH_4 concentration at the dam site of the XLD reservoir was shown in the flood season. However, the peak values of CH_4 concentrations at both the surface and bottom water of the XJB reservoir were observed during the flood season. However, there was no significant difference in CH_4 concentrations between the surface and bottom water. The lowest CO_2 concentration was found before the XJB dam in March, and the CO_2 concentrations in surface water were significantly lower than those in bottom water (Figure 5A, 5B).

Stable carbon isotopic signatures of CH_4 in the water column could help to explore and identify CH_4 production and transformation in reservoirs (Whiticar and Faber, 1986; Lima, 2005; Templeton et al., 2006). $\delta^{13}C\text{-}CH_4$ in all sampling water of both reservoirs ranged from −8.3‰ to −54.0‰ with a mean of −32.7 ± 9.0‰ (SD, n=156, Figure 5). $\delta^{13}C\text{-}CH_4$ in all water samples showed obvious temporal and spatial variations, and maximum values were found before and under the two dams. Lower

https://doi.org/10.5194/bg-2021-234
Preprint. Discussion started: 29 September 2021

367 δ^{13}C-CH_4 values were observed in March and July, where the peak value of CH_4
368 concentrations was found. However, most δ^{13}C-CH_4 in both surface and bottom water
369 from the two reservoirs displayed no significant differences except for that in March
370 from the XJB reservoir (Figure 5A, 5B).

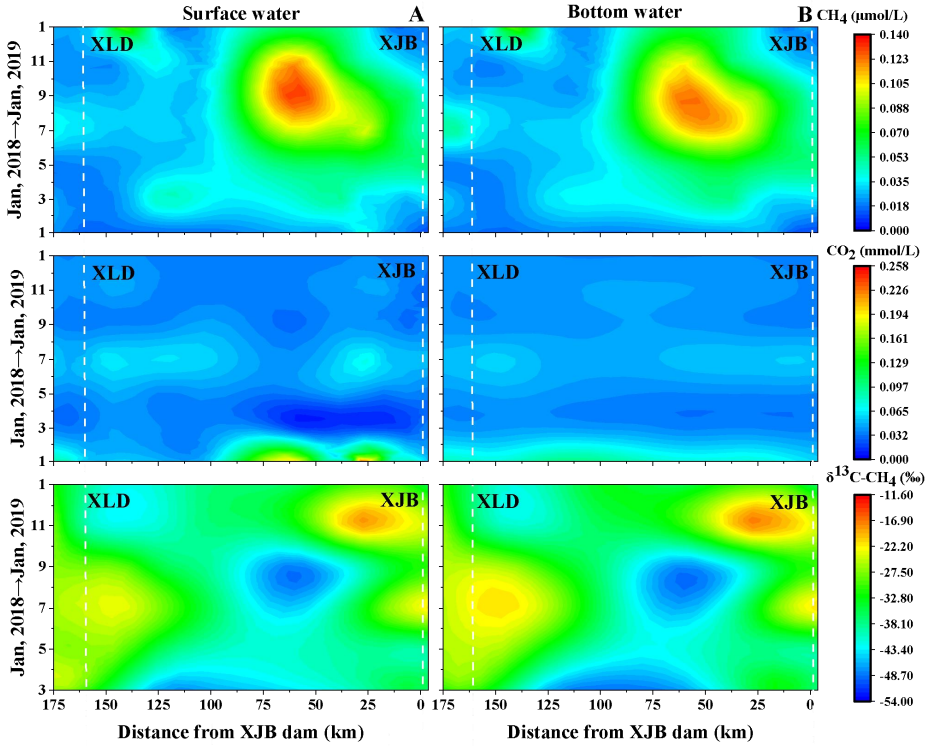

371
372 **Figure 5. Wavelet figure showing the spatial and temporal distributions in CH_4, CO_2 and**
373 **δ^{13}C-CH_4 of the surface (A) and bottom (B) water from the XLD and XJB reservoirs.**

374 In freshwaters, a large fraction of CH_4 in the aquatic food network exists as a
375 carbon source which was oxidized by bacteria, can reduce CH_4 entering the water by
376 diffusion (Jones and Grey, 2011; Taipale et al., 2011; Frossard et al., 2015; Sawakuchi et
377 al., 2016; Matoušů et al., 2019; Thottathil et al., 2019; Saarela et al., 2020), which may
378 change CH_4 dynamics in water. Previous studies reported that the methane oxidizing
379 bacteria (MOB) can survive at oxic-anoxic interfaces in freshwater systems, and CH_4
380 oxidation was frequently found in environments with high CH_4 and DO concentrations
381 (Bagnoud et al., 2020; Reis et al., 2020; Bai et al., 2021). Moreover, the δ^{13}C values of

https://doi.org/10.5194/bg-2021-234
Preprint. Discussion started: 29 September 2021

biogenic methane during methanogenesis were very low, such as methanogenesis by acetate fermentation in freshwaters, and the $\delta^{13}C\text{-}CH_4$ was then gradually elevated during CH_4 oxidation due to ^{13}C enrichment in residual CH_4 (Whiticar and Faber, 1986; Conrad, 1999; Bastviken et al., 2002; Lima, 2005). The magnitude of $\delta^{13}C\text{-}CH_4$ by MOB significantly depends on environmental conditions, so the fractionation factor (**α**) caused by microbial CH_4 oxidation shows a large range of 1.003 to 1.039 (Templeton et al., 2006).

The study area was divided into three sections along longitudinal gradients, B1-B4/L1-L3 as lacustrine regions (before the dam), B5-B7 as transition regions, and X1-X2/B8-B10 as riverine reaches. In this study, there was no apparent anoxic water column in the lacustrine regions (upstream of the dam) of the XJB reservoir. Therefore, the oxic surface sediment and large water depth could have mitigated the release of CH_4 bubbles potentially produced by the deep sediment, which was likely to lead to low CH_4 accumulation in water before the dam. The most $\delta^{13}C\text{-}CH_4$ in the water column were above −50‰ of methanogenesis by acetate fermentation, which indicated that CH_4 was dominantly oxidized in the two reservoirs, especially $\delta^{13}C\text{-}CH_4$ in the lacustrine region, had higher values and was significantly different from riverine reaches and transition regions (Figure S6). Therefore, the CH_4 accumulation in the water column may be influenced by MOB. Significantly, the most CH_4 oxidation process from B6 (the hotspot of CH_4) to B1 (before dam) in the XJB reservoir can also be presented by Rayleigh fractionation, for example, CH_4 concentrations and $\delta^{13}C\text{-}CH_4$ in the March, July, September 2018 and January 2019 satisfied the fractionation caused by microbial CH_4 oxidation, and **α** ranged from 1.01 to 1.035 (Figure S7). The CH_4 oxidation process was interestingly discovered along with the river flow, but the $\delta^{13}C\text{-}CH_4$ in vertical water showed no significant differences. Only the $\delta^{13}C\text{-}CH_4$ in bottom water from the XJB reservoir was significantly lower than that in surface water in March, yet there was no significant difference in CH_4 concentrations (Figure 5). Although recent studies have indicated that the $\delta^{13}C$ values of CH_4 produced in oxic waters are usually less negative than those of CH_4 accumulation in an anaerobic environment (Hartmann et al., 2020),

https://doi.org/10.5194/bg-2021-234
Preprint. Discussion started: 29 September 2021

411 more evidence is needed to support this process in this study.

412 # 4 Discussion

413 ## 4.1 Cascade damming effect on input and accumulation of POC

414 The distribution of POC in a river can be significantly influenced by dams. At first,
415 damming increased losses of river connectivity and reduced water flow in the main
416 channel, which possibly decreased the transport of POC after damming due to the long
417 HRT, further resulting in bulk accumulation and burial of POC in reservoirs (Ulseth and
418 Hall Jr, 2015; Li et al., 2017a; Almeida et al., 2019; Li et al., 2020a; Wang et al., 2020).
419 Additionally, dam construction promotes the intensive water-level fluctuations to cause
420 landslides and debris flows and indirectly influence land types, which may increase the
421 terrestrial POC in the reservoir (Yao et al., 2006; Luo et al., 2016; Iqbal et al., 2018;
422 Zorzal-Almeida et al., 2018).

423 Based on the N/C mole ratios and δ^{13}C-POC values, POC mostly originated from
424 terrestrial POC in the XLD and XJB reservoirs. Water temperature was the only factor
425 that exhibits an obvious positive effect on autochthonous POC (Figure S8), which was
426 mainly caused by the outbreak of algal blooms in spring to increase autochthonous POC
427 in summer (Figure S5). The water level of the XJB reservoir and water flow exhibit a
428 significantly positive effect on terrestrial POC (Figure S8). Due to intensive water-level
429 fluctuations, the high-water level in January was modulated to a low water level in
430 March by reservoir scheduling operation, which led to an increase in the input of
431 terrestrial POC in March (Figure 2C, 2D, S5). Additionally, terrestrial POC in July
432 under high water flow displayed an increasing trend that was possibly affected by runoff
433 erosion. The water level and water flow caused by reservoir scheduling operation were
434 primary factors for the input of terrestrial POC. Meanwhile, due to the low clay content
435 of surface soil in the river basin, the particulate matter derived from soil erosion may
436 have a low OC content (Yu et al., 2011; Wu et al., 2020). This study showed that the
437 proportion of POC in TPM during the flood season was lower than that in the dry
438 season in cascade reservoirs (Figure S9). These results imply that particulate matter

https://doi.org/10.5194/bg-2021-234
Preprint. Discussion started: 29 September 2021

439 from the river basin was less composed of OC, which suggests that a small amount of
440 terrestrial POC possibly enters the XLD and XJB reservoirs during the flood season.
441 The DOC/POC ratios with a global average value of 1-1.2 displayed an
442 exponentially negative correlation with the deposition of particulate matter in major
443 rivers (Ran et al., 2013). In this study, the DOC/POC ratios in March from the XLD and
444 XJB reservoirs with an average value of 3.96 were significantly lower than those in the
445 other months (Figure 6) and close to the Long Chuan River in the Jinsha River Basin
446 (Lu et al., 2012), which suggests that the sedimentation of POC in March was
447 significant. However, the average DOC/POC ratio in the flood period was higher than
448 10, which indicates that the accumulation of POC in the flood period was very low.
449 Because there are no large tributaries in the XJB reservoir, the accumulation of POC
450 from upstream and riverbanks were primarily reflected by the mass balance calculation
451 of POC (Figure 7A). According to the mass balance results of POC, the accumulation of
452 POC was mainly reflected in March (Figure 7A), while the difference in POC flux in
453 July and September during the flood period was not evident. These results also indicate
454 that the accumulation of POC in the XJB reservoir was limited during the flood season.
455 Therefore, the cumulative effect of POC at a bimonthly scale was not significant in the
456 XLD and XJB reservoirs.

https://doi.org/10.5194/bg-2021-234
Preprint. Discussion started: 29 September 2021

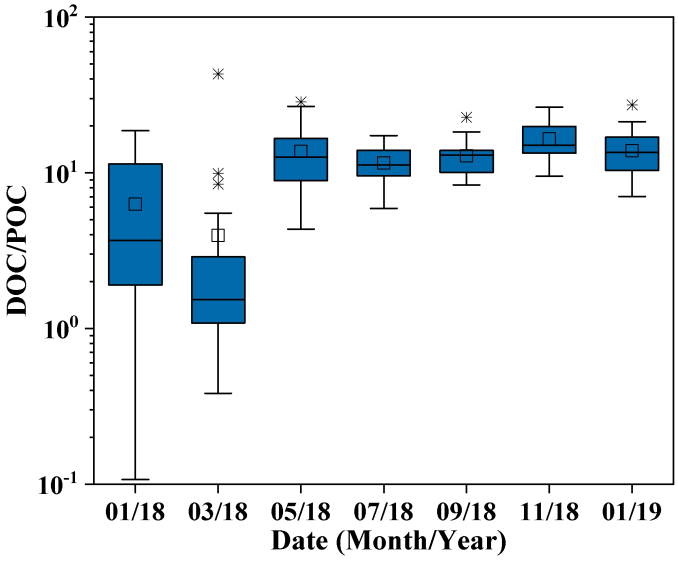

Figure 6. Box plot showing the distribution of DOC/POC ratios in sampling month from the XLD and XJB reservoirs (the asterisks, black squares and middle black lines represented outliers, mean values and medians).

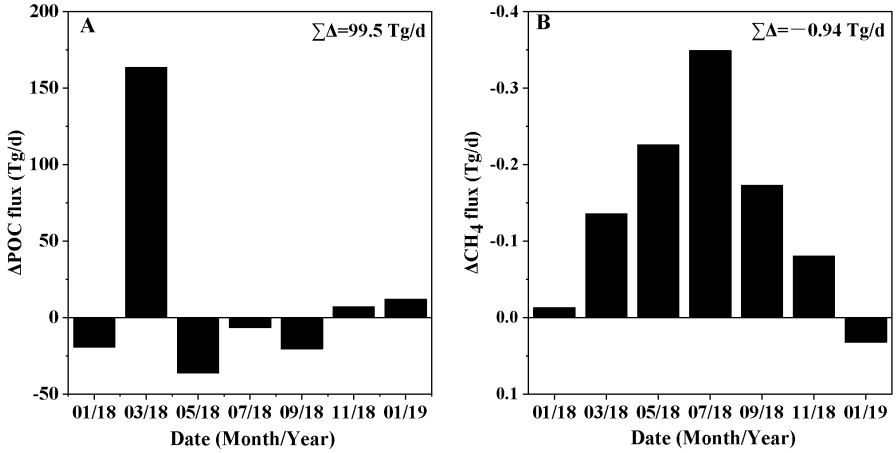

Figure 7. Mass balance calculations of POC (A) and CH_4 (B) in sampling month from the XJB reservoir.

4.2 CH_4 accumulation influenced by terrestrial POC in deep river-valley dammed cascade reservoirs

CH_4 production and emissions in a freshwater system can be affected by parameters such as geography, hydrology, OM, water temperature, and final electron

https://doi.org/10.5194/bg-2021-234
Preprint. Discussion started: 29 September 2021

468 receptors, yet POC was the most important factor for CH_4 accumulation in rivers
469 (Baulch et al., 2011; Crawford et al., 2014; Stanley et al., 2016). The degradation of
470 different sources of POC in freshwaters was different. Autochthonous POC has been
471 found to have a high bioavailability, yet terrestrial POC was already partly degraded and
472 less available for microorganisms (Guillemette et al., 2013). Autochthonous POC can be
473 the main reason for promoting CH_4 production in freshwaters, such as Lake Fuxian and
474 Lake Diamond in the USA (West et al., 2012; Li et al., 2020b). Due to terrestrial POC
475 accounting for large proportions in sediment, terrestrial POC can also have a potential
476 promotion effect on CH_4 accumulation, such as the William H. Harsha reservoir in the
477 USA (Berberich et al., 2020) and the Congo River (Upstill-Goddard et al., 2017).
478 Therefore, the river reservoirs affected by dam interception have complicated
479 hydrological characteristics of lakes and rivers, which results in different impacts of
480 autochthonous and terrestrial POC on CH_4 in reservoirs.

481 Young reservoirs are frequently believed to be significant CH_4 emitters due to the
482 decomposition of flooded OC (Prairie et al., 2018). The structural equation model can
483 be used to explore the relationship between different sources of POC and CH_4 by
484 various physicochemical factors (Figure S8). In terms of exogenous variables, the
485 hydropower production of the XJB reservoir, water temperature and flow show positive
486 correlations, and the water level of the XJB reservoir displayed negative correlations
487 with the hydropower production of the XJB reservoir, water flow, and temperature.
488 Additionally, CH_4 accumulation in deep river-valley dammed cascade reservoirs was
489 positively affected by terrestrial POC, water flow, and temperature rather than
490 autochthonous POC, hydropower production, and the water level of the XJB reservoir
491 (Figure S8). However, this path model cannot illuminate the relationship among CH_4
492 (R^2=0.22), autochthonous (R^2=0.17) and terrestrial POC (R^2=0.11) in the two reservoirs.
493 This implies that the causality among variables in the temporal dimension is not
494 synchronous, and more factors affecting relationships among CH_4 concentration and
495 autochthonous and terrestrial POC in the spatial dimension need to be considered.

496 The dam constructions hindered the water velocity, resulting in increased HRT

https://doi.org/10.5194/bg-2021-234
Preprint. Discussion started: 29 September 2021

(Wang et al., 2020). The relationships among HRT, CH_4 concentration, autochthonous and terrestrial POC are discussed below. The terrestrial POC and CH_4 concentrations in the XLD and XJB reservoirs present single peaks with HRT (Figure 8A, 8C), and autochthonous POC displays a positive correlation with HRT (Figure 8B). HRT as an exogenous variable in the structural equation model, was also used to explain the spatial relationship among endogenous variables such as CH_4 and autochthonous and terrestrial POC (Figure 9). The structural equation model shows a significant positive effect between HRT and autochthonous POC, which can be explained by an increase in phytoplankton photosynthesis (Crawford et al., 2016).

https://doi.org/10.5194/bg-2021-234
Preprint. Discussion started: 29 September 2021

Biogeosciences Discussions Open Access EGU

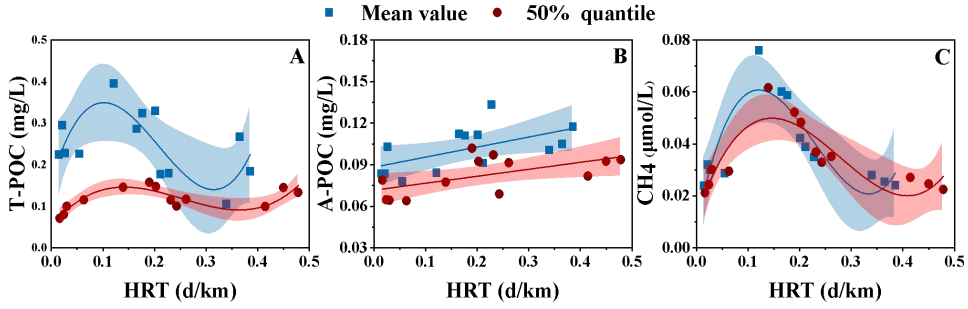

Figure 8. Polynomial and linear fit relationship between POC, CH_4 and HRT in the spatial dimension from the XLD and XJB reservoirs (the blue and red area represented confidence bands and confidence level for curves). The mean values and 50% quantiles of these variables were considered.

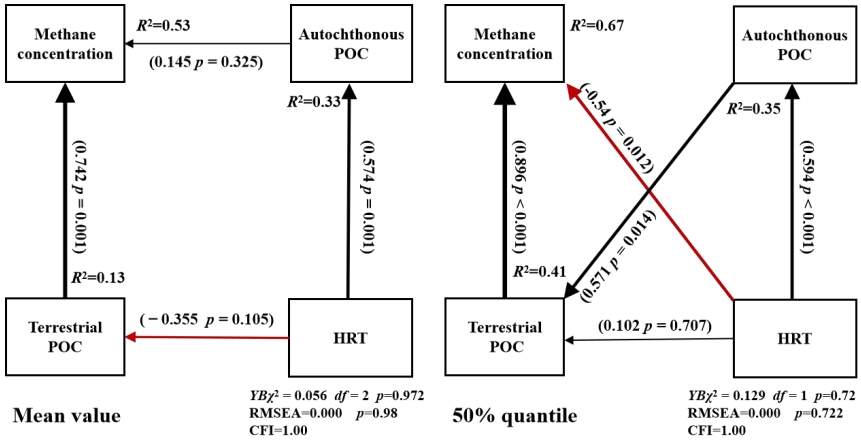

Figure 9. Structural equation model among the mean values (left) and 50% quantiles (right) of HRT, autochthonous POC, terrestrial POC and CH_4 in the spatial dimension from the XLD and XJB reservoirs.

Previous investigations have shown that autochthonous POC in lake reservoirs with depths greater than 100 m was completely mineralized before carbon burial (Steinsberger et al., 2020). Autochthonous POC can be rapidly used to produce CH_4, while the decomposition of terrestrial POC was slower (Grasset et al., 2018; Isidorova et al., 2019). Autochthonous POC can be easily oxidized in deep water columns before entering anaerobic environments or less distributed in surface sediments. Additionally, surface sediments often do not have good stability and an anaerobic environment, which results in autochthonous POC being more likely to be converted to CO_2 (Isidorova et al.,

https://doi.org/10.5194/bg-2021-234
Preprint. Discussion started: 29 September 2021

523 2019). Therefore, it was inferred that autochthonous POC displays no significant
524 relationship with CH_4 in this study.

525 The CH_4 concentrations in the two reservoirs were positively influenced by
526 terrestrial POC (Figure 8, 9). The structural equation model can well explain the
527 relationship with autochthonous POC (R^2=0.33 for mean value, R^2=0.35 for 50%
528 quantile) and CH_4 (R^2=0.53 for mean value, R^2=0.67 for 50% quantile), except for
529 terrestrial POC (R^2=0.13 for mean value, R^2=0.41 for 50% quantile). However,
530 terrestrial POC and CH_4 concentrations display a positive correlation in the spatial
531 dimension (Figure S10). The POC concentrations exhibit an exponential relationship
532 with the contribution of terrestrial POC, which may imply that terrestrial POC was a
533 major input for POC in the XLD and XJB reservoirs (Figure 10). Although the
534 autochthonous POC and CH_4/CO_2 mole ratios in March show a significantly positive
535 relationship mainly due to the outbreak of algal blooms, the most positive relationship
536 between terrestrial POC and CH_4/CO_2 mole ratios also indicates that the input of
537 terrestrial POC in the flood season is a crucial reason for CH_4 production (Figure S11).

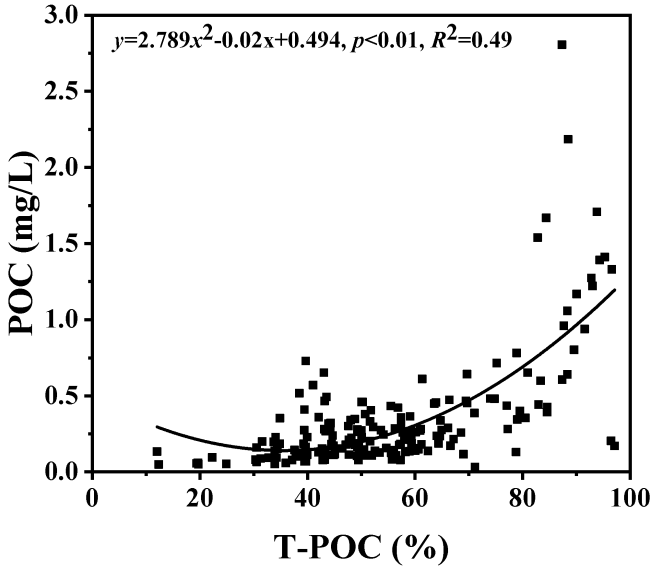

538

539 **Figure 10. Polynomial fit relationship between the contribution of terrestrial POC and POC**
540 **concentrations in the XLD and XJB reservoirs.**

541 The mass balance of CH_4 in the XJB reservoir was related to the estimation of CH_4

https://doi.org/10.5194/bg-2021-234
Preprint. Discussion started: 29 September 2021

production. The annual CH_4 production showed an obvious single peak, and the highest peak value was found in July (Figure 7B). However, there was low accumulation and no significant increasing trend of terrestrial POC during the flood season influenced by cascade damming, which indicates that no large amount of fresh terrestrial POC was decomposed by bacteria to produce more CH_4. Water temperature significantly affects the respiration rate of bacteria and then impacts the degradation of OM. Therefore, CH_4 production in the flood season may be affected by higher water temperatures, which was supported by the structural equation model discussed above (Figure S8) and consistent with previous studies (Delsontro et al., 2010; Beaulieu et al., 2014). However, the difference in temperature from the XLD to XJB reservoirs in July and September was not evident (Figure S3), which means that the CH_4 accumulation in deep river-valley dammed cascade reservoirs is limitedly influenced by water temperature. These results suggest that terrestrial POC was the key factor in CH_4 accumulation in the XLD and XJB reservoirs.

However, there are numerous factors influence carbon migration and transformation in damming rivers. More work needs to be done in the future, such as the contribution of resuspended sediment POC to terrestrial POC. As complicated processes of CH_4 accumulation are influenced by the input of terrestrial POC, more modeling factors need to be considered.

5 Conclusions

POC in the XLD and XJB reservoirs mainly originates from terrestrial POC (56%). CH_4 oxidation potentially influences the variations in CH_4 concentrations and $\delta^{13}C$-CH_4 in cascade reservoirs. Water level variations and flow regulation caused by reservoir operation are primary factors for the input of terrestrial POC. The cumulative effect of POC at a bimonthly scale was not significant in the XLD and XJB reservoirs. Terrestrial POC displays more persistent impacts on CH_4 accumulation. This study provides a scientific basis for revealing the major reason and mechanisms of CH_4 accumulation in high-energy-density reservoirs under reservoir scheduling operation and helps to further

https://doi.org/10.5194/bg-2021-234
Preprint. Discussion started: 29 September 2021

570 understand biogeochemical cycles of carbon in river-reservoir systems.

571 Author contributions

572 YZ and YS contributed equally to this work, processed the data, drew the figures,
573 designed the research framework and wrote the manuscript. ZL designed the study
574 protocol, supervised the study, wrote and revised the manuscript. SG, LL, BZ and YQ
575 carried out the field sampling and analyzed the samples.

576 Competing interests

577 The authors declare that they have no conflict of interest.

578 Acknowledgements

579 The National Natural Science Foundation of China (Project No. 51861125204,
580 51679226 and 42107273) primarily supported this work. The Interdisciplinary Team
581 Project under auspices of "Light of West" Program from Chinese Academy of Sciences
582 partially supported this work. Dr. Zhe Li is also supported by Chongqing Natural
583 Science Funds for Distinguished Young Scientists (Project No. cstc2020jcyj-jqX0010).
584 We thank the China Three Gorges Corporation for providing partial funding support for
585 monthly sampling and daily hydrological data. We also thank Ms. Yinmin Xuan and Mr.
586 Hailong Du who participated field sampling campaigns.

587 References

588 Abril, G., Guérin, F., Richard, S., Delmas, R., Galy - Lacaux, C., Gosse, P., Tremblay, A., Varfalvy, L.,
589 Dos Santos, M. A., and Matvienko, B.: Carbon dioxide and methane emissions and the carbon
590 budget of a 10 - year old tropical reservoir (Petit Saut, French Guiana), Global Biogeochem Cy,
591 19, 2005.
592 Almeida, R. M., Hamilton, S. K., Rosi, E. J., Arantes, J. D., Barros, N., Boemer, G., Gripp, A., Huszar, V.
593 L., Junger, P. C., and Lima, M.: Limnological effects of a large Amazonian run-of-river dam on
594 the main river and drowned tributary valleys, Sci Rep-UK, 9, 1-11, 2019.
595 Bagnoud, A., Pramateftaki, P., Bogard, M. J., Battin, T. J., and Peter, H.: Microbial ecology of
596 methanotrophy in streams along a gradient of CH4 availability, Front Microbiol, 11, 771, 2020.
597 Bai, X., Xu, Q., Li, H., Cheng, C., and He, Q.: Lack of methane hotspot in the upstream dam: Case study
598 in a tributary of the Three Gorges Reservoir, China, Sci Total Environ, 754, 142151, 2021.
599 Bastviken, D., Ejlertsson, J., and Tranvik, L.: Measurement of methane oxidation in lakes: a comparison
600 of methods, Environ Sci Technol, 36, 3354-3361, 2002.

https://doi.org/10.5194/bg-2021-234
Preprint. Discussion started: 29 September 2021

601 Baulch, H. M., Dillon, P. J., Maranger, R., and Schiff, S. L.: Diffusive and ebullitive transport of methane
602 and nitrous oxide from streams: Are bubble-mediated fluxes important?, J Geophys Res:Biogeo,
603 116, 2011.
604 Beaulieu, J. J., Smolenski, R. L., Nietch, C. T., Townsend-Small, A., and Elovitz, M. S.: High methane
605 emissions from a midlatitude reservoir draining an agricultural watershed, Environ Sci Technol,
606 48, 11100-11108, 2014.
607 Berberich, M. E., Beaulieu, J. J., Hamilton, T. L., Waldo, S., and Buffam, I.: Spatial variability of
608 sediment methane production and methanogen communities within a eutrophic reservoir:
609 Importance of organic matter source and quantity, Limnol Oceanogr, 65, 1336-1358, 2020.
610 Chen, J., Yang, H., Zeng, Y., Guo, J., Song, Y., and Ding, W.: Combined use of radiocarbon and stable
611 carbon isotope to constrain the sources and cycling of particulate organic carbon in a large
612 freshwater lake, China, Sci Total Environ, 625, 27-38, 2018a.
613 Chen, X., Feng, M., Ke, F., Pan, J., Fan, F., Wang, Y., and Li, W.: Source and biogeochemical distribution
614 of organic matter in surface sediment in the deep oligotrophic Lake Fuxian, China, Aquat
615 Geochem, 24, 55-77, 2018b.
616 Ciais, P., Sabine, C., Bala, G., Bopp, L., Brovkin, V., Canadell, J., Chhabra, A., DeFries, R., Galloway, J.,
617 and Heimann, M.: Carbon and other biogeochemical cycles, in: Climate change 2013: the
618 physical science basis. Contribution of Working Group I to the Fifth Assessment Report of the
619 Intergovernmental Panel on Climate Change, Cambridge University Press, 465-570, 2014.
620 Conrad, R.: Contribution of hydrogen to methane production and control of hydrogen concentrations in
621 methanogenic soils and sediments, Fems Microbiol Ecol, 28, 193-202, 1999.
622 Crawford, J. T., Loken, L. C., Stanley, E. H., Stets, E. G., Dornblaser, M. M., and Striegl, R. G.: Basin
623 scale controls on CO2 and CH4 emissions from the Upper Mississippi River, Geophys Res Lett,
624 43, 1973-1979, 2016.
625 Crawford, J. T., Lottig, N. R., Stanley, E. H., Walker, J. F., Hanson, P. C., Finlay, J. C., and Striegl, R. G.:
626 CO2 and CH4 emissions from streams in a lake-rich landscape: Patterns, controls, and regional
627 significance, Global Biogeochem Cy, 28, 197-210, 2014.
628 de Castro Bueno, C., Frascareli, D., Gontijo, E. S., van Geldern, R., Rosa, A. H., Friese, K., and Barth, J.
629 A.: Dominance of in situ produced particulate organic carbon in a subtropical reservoir inferred
630 from carbon stable isotopes, Sci Rep-UK, 10, 1-11, 2020.
631 Deemer, B. R., Harrison, J. A., Li, S., Beaulieu, J. J., DelSontro, T., Barros, N., Bezerra-Neto, J. F.,
632 Powers, S. M., Dos Santos, M. A., and Vonk, J. A.: Greenhouse gas emissions from reservoir
633 water surfaces: a new global synthesis, Bioscience, 66, 949-964, 2016.
634 DelSontro, T., McGinnis, D. F., Sobek, S., Ostrovsky, I., and Wehrli, B.: Extreme methane emissions
635 from a Swiss hydropower reservoir: contribution from bubbling sediments, Environ Sci Technol,
636 44, 2419-2425, 2010.
637 Deng, H., Li, Y., Liu, M., Duan, X., Liu, S., and Chen, D.: Stable isotope analysis reveals the importance
638 of riparian resources as carbon subsidies for fish species in the Daning River, a tributary of the
639 Three Gorges Reservoir, China, Water, 10, 1233, 2018.
640 Dlugokencky, E. J.: Trends in atmospheric methane, NOAA/GML
641 (www.esrl.noaa.gov/gmd/ccgg/trends_ch4/), 2021.
642 Frossard, V., Verneaux, V., Millet, L., Magny, M., and Perga, M.-E.: Changes in carbon sources fueling
643 benthic secondary production over depth and time: coupling Chironomidae stable carbon
644 isotopes to larval abundance, Oecologia, 178, 603-614, 2015.

https://doi.org/10.5194/bg-2021-234
Preprint. Discussion started: 29 September 2021

645 Grasset, C., Mendonça, R., Villamor Saucedo, G., Bastviken, D., Roland, F., and Sobek, S.: Large but
646 variable methane production in anoxic freshwater sediment upon addition of allochthonous and
647 autochthonous organic matter, Limnol Oceanogr, 63, 1488-1501, 2018.
648 Guillemette, F., McCallister, S. L., and del Giorgio, P. A.: Differentiating the degradation dynamics of
649 algal and terrestrial carbon within complex natural dissolved organic carbon in temperate lakes, J
650 Geophys Res:Biogeo, 118, 963-973, 2013.
651 Hartmann, J. F., Günthel, M., Klintzsch, T., Kirillin, G., Grossart, H.-P., Keppler, F., and
652 Isenbeck-Schröter, M.: High spatiotemporal dynamics of methane production and emission in
653 oxic surface water, Environ Sci Technol, 54, 1451-1463, 2020.
654 Iqbal, J., Dai, F., Hong, M., Tu, X., and Xie, Q.: Failure mechanism and stability analysis of an active
655 landslide in the xiangjiaba reservoir area, southwest china, J Earth Sci, 29, 646-661, 2018.
656 Isidorova, A., Mendonça, R., and Sobek, S.: Reduced mineralization of terrestrial OC in anoxic sediment
657 suggests enhanced burial efficiency in reservoirs compared to other depositional environments, J
658 Geophys Res:Biogeo, 124, 678-688, 2019.
659 Jiang, Y. and Ji, H.: Isotopic indicators of source and fate of particulate organic carbon in a karstic
660 watershed on the Yunnan-Guizhou Plateau, Appl Geochem, 36, 153-167, 2013.
661 Jones, R. I. and Grey, J.: Biogenic methane in freshwater food webs, Freshwater Biol, 56, 213-229, 2011.
662 Kang, S., Kim, J.-H., Kim, D., Song, H., Ryu, J.-S., Ock, G., and Shin, K.-H.: Temporal variation in
663 riverine organic carbon concentrations and fluxes in two contrasting estuary systems: Geum and
664 Seomjin, South Korea, Environ Int, 133, 105126, 2019.
665 Kendall, C., Silva, S. R., and Kelly, V. J.: Carbon and nitrogen isotopic compositions of particulate
666 organic matter in four large river systems across the United States, Hydrol Process, 15,
667 1301-1346, 2001.
668 Li, M., Peng, C., Wang, M., Xue, W., Zhang, K., Wang, K., Shi, G., and Zhu, Q.: The carbon flux of
669 global rivers: A re-evaluation of amount and spatial patterns, Ecol Indic, 80, 40-51, 2017a.
670 Li, Z., Du, H., Xiao, Y., and Guo, J.: Carbon footprints of two large hydro-projects in China: Life-cycle
671 assessment according to ISO/TS 14067, Renew Energ, 114, 534-546, 2017b.
672 Li, Z., Lu, L., Lv, P., Zhang, Z., and Guo, J.: Imbalanced stoichiometric reservoir sedimentation regulates
673 methane accumulation in China's Three Gorges Reservoir, Water Resour Res, 56,
674 e2019WR026447, 2020a.
675 Li, Z., Li, X., Wang, X., Ma, J., Xu, J., Xu, X., Han, R., Zhou, Y., Yan, X., and Wang, G.: Isotopic
676 evidence revealing spatial heterogeneity for source and composition of sedimentary organic
677 matters in Taihu Lake, China, Ecol Indic, 109, 105854, 2020b.
678 Lima, I. B. T.: Biogeochemical distinction of methane releases from two Amazon hydroreservoirs,
679 Chemosphere, 59, 1697-1702, 2005.
680 Lu, X., Li, S., He, M., Zhou, Y., Li, L., and Ziegler, A. D.: Organic carbon fluxes from the upper Yangtze
681 basin: an example of the Longchuanjiang River, China, Hydrol Process, 26, 1604-1616, 2012.
682 Luo, Z., Ma, J.-M., Zheng, S.-L., Nan, C.-Z., and Nie, L.-M.: Different hydrodynamic conditions on the
683 deposition of organic carbon in sediment of two reservoirs, Hydrobiologia, 765, 15-26, 2016.
684 Matoušů, A., Rulík, M., Tušer, M., Bednařík, A., Šimek, K., and Bussmann, I.: Methane dynamics in a
685 large river: a case study of the Elbe River, Aquat Sci, 81, 1-15, 2019.
686 Muller, M.: Dams have the power to slow climate change, Nature, 566, 315-317, 2019.
687 Parnell, A. C., Inger, R., Bearhop, S., and Jackson, A. L.: Source partitioning using stable isotopes: coping
688 with too much variation, PloS one, 5, e9672, 2010.

https://doi.org/10.5194/bg-2021-234
Preprint. Discussion started: 29 September 2021

689 Parnell, A. C., Phillips, D. L., Bearhop, S., Semmens, B. X., Ward, E. J., Moore, J. W., Jackson, A. L.,
690 Grey, J., Kelly, D. J., and Inger, R.: Bayesian stable isotope mixing models, Environmetrics, 24,
691 387-399, 2013.
692 Prairie, Y. T., Alm, J., Beaulieu, J., Barros, N., Battin, T., Cole, J., Del Giorgio, P., DelSontro, T., Guérin,
693 F., and Harby, A.: Greenhouse gas emissions from freshwater reservoirs: what does the
694 atmosphere see?, Ecosystems, 21, 1058-1071, 2018.
695 Ran, L., Lu, X., Sun, H., Han, J., Li, R., and Zhang, J.: Spatial and seasonal variability of organic carbon
696 transport in the Yellow River, China, J Hydrol, 498, 76-88, 2013.
697 Reis, P. C., Ruiz-González, C., Crevecoeur, S., Soued, C., and Prairie, Y. T.: Rapid shifts in
698 methanotrophic bacterial communities mitigate methane emissions from a tropical hydropower
699 reservoir and its downstream river, Sci Total Environ, 748, 141374, 2020.
700 Rosentreter, J. A., Borges, A. V., Deemer, B. R., Holgerson, M. A., Liu, S., Song, C., Melack, J.,
701 Raymond, P. A., Duarte, C. M., and Allen, G. H.: Half of global methane emissions come from
702 highly variable aquatic ecosystem sources, Nat Geosci, 14, 225-230, 2021.
703 Ru, H., Li, Y., Sheng, Q., Zhong, L., and Ni, Z.: River damming affects energy flow and food web
704 structure: A case study from a subtropical large river, Hydrobiologia, 847, 679-695, 2020.
705 Saarela, T., Rissanen, A. J., Ojala, A., Pumpanen, J., Aalto, S. L., Tiirola, M., Vesala, T., and Jäntti, H.:
706 CH 4 oxidation in a boreal lake during the development of hypolimnetic hypoxia, Aquat Sci, 82,
707 1-12, 2020.
708 Saunois, M., Bousquet, P., Poulter, B., Peregon, A., Ciais, P., Canadell, J. G., Dlugokencky, E. J., Etiope,
709 G., Bastviken, D., and Houweling, S.: The global methane budget 2000–2012, Earth Syst Sci
710 Data, 8, 697-751, 2016.
711 Saunois, M., Stavert, A. R., Poulter, B., Bousquet, P., Canadell, J. G., Jackson, R. B., Raymond, P. A.,
712 Dlugokencky, E. J., Houweling, S., and Patra, P. K.: The global methane budget 2000–2017,
713 Earth Syst Sci Data, 12, 1561-1623, 2020.
714 Sawakuchi, H. O., Bastviken, D., Sawakuchi, A. O., Ward, N. D., Borges, C. D., Tsai, S. M., Richey, J. E.,
715 Ballester, M. V. R., and Krusche, A. V.: Oxidative mitigation of aquatic methane emissions in
716 large Amazonian rivers, Global Change Biol, 22, 1075-1085, 2016.
717 Shi, W., Chen, Q., Yi, Q., Yu, J., Ji, Y., Hu, L., and Chen, Y.: Carbon emission from cascade reservoirs:
718 spatial heterogeneity and mechanisms, Environ Sci Technol, 51, 12175-12181, 2017.
719 Stanley, E. H., Casson, N. J., Christel, S. T., Crawford, J. T., Loken, L. C., and Oliver, S. K.: The ecology
720 of methane in streams and rivers: patterns, controls, and global significance, Ecol Monogr, 86,
721 146-171, 2016.
722 Steinsberger, T., Schwefel, R., Wüest, A., and Müller, B.: Hypolimnetic oxygen depletion rates in deep
723 lakes: Effects of trophic state and organic matter accumulation, Limnol Oceanogr, 65, 3128-3138,
724 2020.
725 Suzuki, K. W., Ueda, H., Nakayama, K., and Tanaka, M.: Spatiotemporal dynamics of stable carbon
726 isotope ratios in two sympatric oligohaline copepods in relation to the estuarine turbidity
727 maximum (Chikugo River, Japan): implications for food sources, J Plankton Res, 36, 461-474,
728 2014.
729 Taipale, S., Kankaala, P., Hahn, M. W., Jones, R. I., and Tiirola, M.: Methane-oxidizing and
730 photoautotrophic bacteria are major producers in a humic lake with a large anoxic hypolimnion,
731 Aquat Microb Ecol, 64, 81-95, 2011.
732 Templeton, A. S., Chu, K.-H., Alvarez-Cohen, L., and Conrad, M. E.: Variable carbon isotope

https://doi.org/10.5194/bg-2021-234
Preprint. Discussion started: 29 September 2021

733 fractionation expressed by aerobic CH4-oxidizing bacteria, Geochim Cosmochim Ac, 70,
734 1739-1752, 2006.
735 Thottathil, S. D., Reis, P. C., and Prairie, Y. T.: Methane oxidation kinetics in northern freshwater lakes,
736 Biogeochemistry, 143, 105-116, 2019.
737 Tittel, J., Hüls, M., and Koschorreck, M.: Terrestrial vegetation drives methane production in the
738 sediments of two German reservoirs, Sci Rep-UK, 9, 1-10, 2019.
739 Ulseth, A. and Hall Jr, R.: Dam tailwaters compound the effects of reservoirs on the longitudinal transport
740 of organic carbon in an arid river, Biogeosciences, 12, 4345-4359, 2015.
741 UNESCO/IHA: GHG measurement guidlines for freshwater reservoirs, UNESCO, The International
742 Hydropower As Sociation (IHA), 138, 2010.
743 Upstill-Goddard, R. C., Salter, M. E., Mann, P. J., Barnes, J., Poulsen, J., Dinga, B., Fiske, G. J., and
744 Holmes, R. M.: The riverine source of CH 4 and N 2 O from the Republic of Congo, western
745 Congo Basin, Biogeosciences, 14, 2267-2281, 2017.
746 Wang, J., Gu, B., Huang, J., Han, X., Lin, G., Zheng, F., and Li, Y.: Terrestrial contributions to the aquatic
747 food web in the middle Yangtze River, PloS one, 9, e102473, 2014.
748 Wang, W., Yi, Y., Zhong, J., Kumar, A., and Li, S.-L.: Carbon biogeochemical processes in a subtropical
749 karst river–reservoir system, J Hydrol, 591, 125590, 2020.
750 WEF and APHA: Standard methods for the examination of water and wastewater, American Public
751 Health Association (APHA): Washington, DC, USA, 2005.
752 West, W. E., Coloso, J. J., and Jones, S. E.: Effects of algal and terrestrial carbon on methane production
753 rates and methanogen community structure in a temperate lake sediment, Freshwater Biol, 57,
754 949-955, 2012.
755 Whiticar, M. J. and Faber, E.: Methane oxidation in sediment and water column environments—isotope
756 evidence, Org Geochem, 10, 759-768, 1986.
757 Wilkinson, J., Bodmer, P., and Lorke, A.: Methane dynamics and thermal response in impoundments of
758 the Rhine River, Germany, Sci Total Environ, 659, 1045-1057, 2019.
759 Wu, Y., Fang, H., Huang, L., and Cui, Z.: Particulate organic carbon dynamics with sediment transport in
760 the upper Yangtze River, Water Res, 184, 116193, 2020.
761 Wu, Y., Zhang, J., Liu, S., Zhang, Z., Yao, Q., Hong, G., and Cooper, L.: Sources and distribution of
762 carbon within the Yangtze River system, Estuarine, Coastal and Shelf Science, 71, 13-25, 2007.
763 Xuan, Y., Tang, C., Cao, Y., Li, R., and Jiang, T.: Isotopic evidence for seasonal and long-term C and N
764 cycling in a subtropical basin of southern China, J Hydrol, 577, 123926, 2019.
765 Yao, Y., Zhang, B., Ma, X., and Ma, P.: Large-scale hydroelectric projects and mountain development on
766 the upper Yangtze river, Mt Res Dev, 26, 109-114, 2006.
767 Yu, H., Wu, Y., Zhang, J., Deng, B., and Zhu, Z.: Impact of extreme drought and the Three Gorges Dam
768 on transport of particulate terrestrial organic carbon in the Changjiang (Yangtze) River, J
769 Geophys Res: Earth, 116, 2011.
770 Zorzal-Almeida, S., Salim, A., Andrade, M. R. M., de Novaes Nascimento, M., Bini, L. M., and Bicudo,
771 D. C.: Effects of land use and spatial processes in water and surface sediment of tropical
772 reservoirs at local and regional scales, Sci Total Environ, 644, 237-246, 2018.
773